IMMUNOBIOLOGY AND IMMUNOTHERAPY

Aberrant function of pathogenic STAT3 mutant proteins is linked to altered stability of monomers and homodimers

Moses M. Kasembeli,[1] Efiyenia Kaparos,[1] Uddalak Bharadwaj,[1] Ahmad Allaw,[1] Alain Khouri,[1] Bianca Acot,[1] and David J. Tweardy[1,2]

[1]Department of Infectious Diseases, Infection Control and Employee Health, and [2]Department of Molecular and Cellular Oncology, The University of Texas MD Anderson Cancer Center, Houston, TX

KEY POINTS

- **Altered stability of STAT3 protein is linked to the molecular pathogenesis of diseases caused by STAT3 SH2D LOF and GOF mutations.**

- **The STAT3 inhibitor TTI-101 reduced pY-peptide binding and cell growth driven by cancer-causing STAT3 SH2D GOF mutants.**

STAT3 mutations, predominantly in the DNA-binding domain (DBD) and Src-homology 2 domain (SH2D), cause rare cases of immunodeficiency, malignancy, and autoimmunity. The exact mechanisms by which these mutations abrogate or enhance STAT3 function are not completely understood. Here, we examined how loss-of-function (LOF) and gain-of-function (GOF) STAT3 mutations within the DBD and SH2D affect monomer and homodimer protein stability as well as their effect on key STAT3 activation events, including recruitment to phosphotyrosine (pY) sites within peptide hormone receptors, tyrosine phosphorylation at Y705, dimerization, nuclear translocation, and DNA binding. The DBD LOF mutants showed reduced DNA binding when homodimerized, whereas the DBD GOF mutants showed increased DNA binding. DBD LOF and GOF mutants showed minimal changes in other STAT3 functions or in monomer or homodimer protein stability. However, SH2D LOF mutants demonstrated reduced conformational stability as either monomers or homodimers, leading to decreased pY-peptide recruitment, tyrosine phosphorylation, dimerization, nuclear localization, and DNA binding. In contrast, cancer-causing SH2D GOF mutants showed increased STAT3 homodimer stability, which increased their DNA binding. Of note, a small-molecule inhibitor of STAT3 that targets the tyrosine phosphopeptide–binding pocket within the STAT3 SH2D potently inhibited cell proliferation driven by STAT3 SH2D GOF mutants. These findings indicate that the stability of STAT3 protein monomer and homodimer is critical for the pathogenesis of diseases caused by SH2D LOF and GOF mutations and suggest that agents that modulate STAT3 monomer and/or homodimer protein stability may have therapeutic value in diseases caused by these mutations.

Introduction

STAT3 participates in the signal transduction pathways of many cytokines, hormones, growth factors, and chemokines[1,2] that are central to multiple cellular processes, including cell growth and survival, as well as adaptive and innate immunity.[3,4] The duration, intensity, and location of STAT3 signaling are carefully calibrated to meet the demands of the cell in response to its environment. Dysregulation of STAT3 signaling has been implicated in multiple diseases, including cancer and immune-related disorders.

STAT3 is organized into 6 functional domains,[5] each of which contributes to its signaling functions (Figure 1A). Adaptive signal transduction depends on posttranslational modifications of STAT3 at key residues, notably phosphorylation at Y705

within the SH2 subdomain, here referred to as the "loop." The loop promotes STAT3 homodimers through reciprocal loop-SH2 interactions.[1] Homodimerization drives nuclear accumulation and alters gene transcription.

In recent years, STAT3 mutations, particularly in the DNA-binding domain (DBD) and Src-homology 2 domain (SH2D), have been shown to disrupt the dynamic connection between the physiologic demands of a cell and STAT3 signaling. Monoallelic germ line loss-of-function (LOF) mutations that reduce STAT3 signaling cause a rare heritable form of primary immune deficiency known as Job's syndrome or autosomal dominant hyper-IgE syndrome (AD-HIES).[6] In contrast, monoallelic somatic or germ line gain-of-function (GOF) STAT3 mutations that increase STAT3 signaling have been identified in patients with lymphoproliferative disorders and early-onset multiorgan autoimmunity, respectively.[7-11]
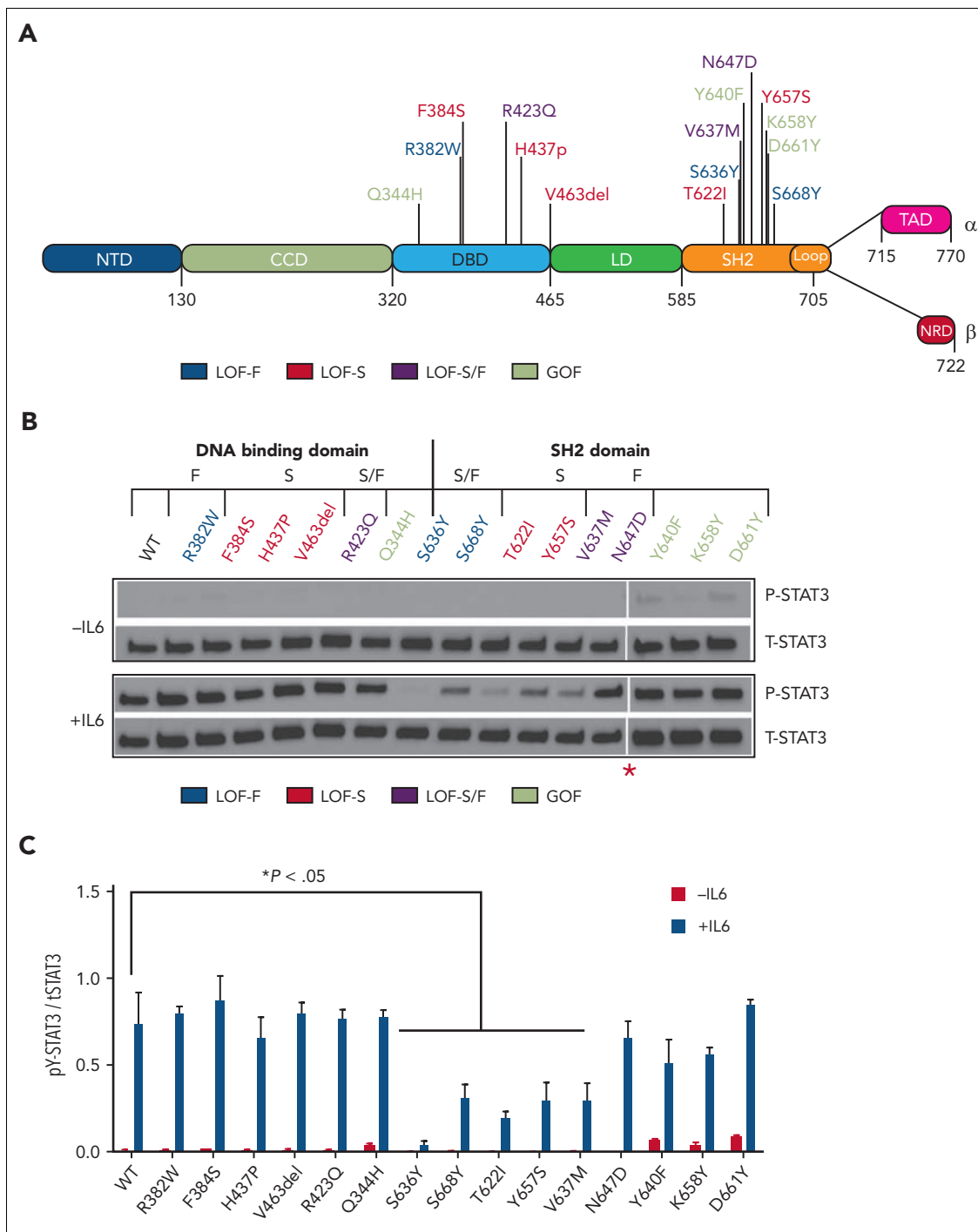
Figure 1. Effect of mutations on cytokine-induced STAT3 Y705 phosphorylation. (A) Schematic diagram of STAT3 depicting each domain: NTD, CCD, DBD, LD, SH2D, TAD, and NRD. (B) Representative immunoblot analysis of lysates of STAT3$^{-/-}$ MEF cells reconstituted with WT or mutant STAT3 constructs and incubated without (top) or with (bottom) IL6/sIL6R (100 ng/mL). Blots were probed with antibody against total (t) STAT3 or pY-STAT, as indicated. The red asterisk (*) indicates that the images are a composite of 2 separate blots imaged simultaneously with equal exposure. (C) Bar graph showing the densitometry signal for pY-STAT3 normalized for total (t) STAT3 and the mean ± SEM of 3 immunoblots shown (*P < .05; Student t test). CCD, coil-coiled domain; LD, linker domain; NRD, nuclear retention domain; NTD, N-terminal domain; SEM, standard error of the mean; TAD, transactivation domain.

Detailed examination of STAT3 mutations that affect its structure and/or functions has provided some insights into the structure and function of this critical signaling protein. We previously showed that proper folding and conformational stability of STAT3 is critical for its function and that mammalian cells rely on several chaperones to achieve this goal.[12] Protein half-life studies

confirmed that mutations predicted by computational modeling to destabilize STAT3 reduced mutant protein half-life in B cells derived from patients with AD-HIES. Importantly, we showed increased STAT3 protein half-life and function in cells heterozygous for structural and structural-functional STAT3 LOF mutations that were treated with small-molecule proteostasis modulators.[13]

Although several studies have provided biochemical insights into the effect of mutations on STAT3 signaling,[14-19] a detailed understanding of how these mutations disrupt or enhance STAT3 function is lacking. Using a combination of biochemical and biophysical assays along with cell-based techniques, we show that LOF and GOF mutations in the DBD of STAT3 lead to decreased or increased DNA binding, respectively. In contrast, LOF mutations within the SH2D affected the overall conformational stability of STAT3 monomers and homodimers, resulting in decreased recruitment, tyrosine phosphorylation, dimerization, nuclear accumulation, and DNA binding of STAT3. In contrast, cancer-causing GOF mutations within SH2D increased the stability of STAT3 homodimers, leading to increased DNA-binding activity. Of note, a small-molecule STAT3 inhibitor, TTI-101, that targets the tyrosine phosphopeptide (pY-peptide)–binding pocket within the STAT3 SH2D and has entered phase II testing in patients with cancer, potently inhibited cell proliferation driven by GOF STAT3 mutants.

Material and methods

Site-directed mutagenesis and plasmid constructs

We used 2 STAT3 constructs: full-length STAT3α and a core STAT3 construct (residues 127-722), described in Backer et al.[20] The full-length STAT3α construct was used in all cell-based assays. Because the full-length STAT3α is not readily amenable to solution-based biophysical and biochemical studies, we used the core construct of STAT3 (127-722), which contains the functional domains necessary to address the major questions asked in this study.[5] For this study, we generated a wild-type (WT) STAT3 construct and 15 STAT3 mutant constructs that were disease-causing, of which 11 were LOF mutations that caused AD-HIES, and 4 were GOF mutations that caused auto-immunity or cancer (Figure 1A and supplemental Figure 1; supplemental Table 1, available on the *Blood* website). Mutations were selected based on their potential impact on the structure and/or function of STAT3, as described in the supplemental Methods. Full-length STAT3α constructs used for mammalian expression were cloned into EX-Z2835-M02 (Genecopoea) or pAcGFP1-C1 (Takara). STAT3 (127-722) constructs used for bacterial expression were cloned into pET15b (Novagen). Each mutant STAT3 construct was generated from the WT construct using the QuikChange II XL Site-Directed Mutagenesis Kit following the manufacturer's protocol (Agilent technologies).

Cell culture, transfections, and treatments

STAT3-deficient murine embryonic fibroblasts (STAT3$^{-/-}$ MEF)[21] were cultured in Dulbecco's modified Eagle medium containing Glutamax (Thermo Fisher Scientific, MA), 10% Hi-FBS (Thermo Fisher Scientific), and 1× Anti-Anti (Thermo Fisher Scientific) at 37°C in an atmosphere containing 5% CO_2 and 90% humidity. STAT3$^{-/-}$ MEF cells ($3.0 × 10^5$) were transfected with plasmid (3 ug) containing STAT3 WT or mutant constructs using the JetPRIME kit (Polyplus Transfection). STAT3$^{-/-}$ MEF cells transfected with WT or each of the 15 mutant constructs expressed STAT3 protein at similar levels. After 24 hours, cells were stimulated with or without IL6 and IL6sR (@ 100 ng/mL) for 30 minutes, washed with phosphate-buffered saline, and lysed as indicated below. Protein concentrations were measured using a Pierce BCA kit (Thermo Scientific).

Phosphotyrosine (pY) peptide pull-down assay

Lysates used for pY-peptide pull-down assays were generated by sonication in a buffer containing 20 mM HEPES (pH7.4), 100 mM NaCl, 0.5% NP40, 1× protease inhibitor cocktail (Roche), and 1× Phosphostop (Roche). N-terminal biotinylated dodecapeptides based on and encompassing Y1068 within the EGFR were synthesized with and without the phosphate moiety at Y1068,[22] immobilized onto neutravidin agarose beads (Pierce), and analyzed as described in the supplemental Methods.

STAT3 DNA-binding assay

Whole cell lysates were prepared in RIPA buffer containing protease and phosphatase inhibitor cocktails (Roche), normalized to total (t) STAT3 protein signal (~10 µg per well) determined by immunoblotting or Luminex bead assays, and used to measure DNA-binding activity using the TransAM STAT3 kit following the manufacturer's protocol (Active Motif, Carlsbad, CA).

Bioluminescence resonance energy transfer (BRET) assay

Cells were transfected with NLuc–STAT3–FlAsH (NSF) or control construct (NS) and labeled with a fluorescein arsenical short hairpin (FlAsH) probe using the TC-FlAsH II In-Cell Tetracysteine Tag Detection Kit following the manufacturer's protocol (Thermo Fisher Scientific). Labeled cells were analyzed for BRET signal in the presence or absence of IL6/IL6sR, as described in the supplemental Methods.

Surface plasmon resonance (SPR) assays for pY-peptide and DNA binding

A Biacore 3000 instrument (GE-Healthcare) was used to measure the binding affinities of recombinant monomer proteins to immobilized phosphorylated EGFR peptide (pY1068) pY-peptide and the binding affinities of recombinant homodimers to hSIE DNA duplex DNA. The assay was performed as published.[23,24] Additional methods for expression and purification of all STAT3 proteins and the SPR binding assays are provided in the supplemental Methods.

Fluorescence microscopy and image analysis

STAT3$^{-/-}$ MEF cells were seeded on CELLview slides (Greiner Bio-One) and incubated for 12 hours before being transiently transfected with Ac-GFP1 STAT3 WT and mutant constructs using the JetPRIME kit (Polyplus Transfection) following the manufacturer's instructions. After 48 hours of incubation, the cells were treated with IL6/IL6R (@ 100 ng/mL) for 30 minutes. The cells were then washed with ice-cold phosphate-buffered saline and fixed in 4% paraformaldehyde. Fluorescence images for GFP, 4′,6-diamidino-2-phenylindole (DAPI), and bright field were acquired on the same field using the BZ-X700-All-in-One fluorescence microscope (Keyence). DAPI images were used to generate a mask for the nucleus using the FIJI package of Image J; bright field images were used to segment and generate a mask for the total cell area. The percent nuclear fluorescence (% NF) was determined in 30 to 40 randomly selected cells by dividing the fluorescence intensity in the nucleus by the fluorescence intensity in the whole cell and multiplying by 100. Each experiment was performed in triplicate.

TTI-101 inhibition of STAT3-dependent growth

STAT3$^{-/-}$ MEFs stably transfected with AcGFP1 WT-STAT3 construct (WT) or STAT3 SH2D GOF mutant D661Y construct or empty vector were serum starved for 24 hours, then incubated in DMEM media with reduced serum (0.5% fetal bovine serum [FBS]) or no serum (0% FBS) without or with TTI-101 (0, 0.1, 0.3, 1, 3, 10, and 100 µM) for 80 hours, and cell viability was assessed by 3-[4,5-dimethylthiazol-2-yl]-2,5-diphenyltetrazolium bromide (MTT) assay. Relative cell growth was calculated by dividing the optical density (OD) values after 80 hours by the OD values after 24 hours of starvation (0 day or t$_0$). Relative % viability was calculated as viability after treatment ÷ viability of untreated cells × 100. IC$_{50}$ values were calculated using GraphPad.

Statistical analysis

Unless otherwise indicated, the results shown are mean ± standard deviation, and difference between means was determined using Student t test as a part of the Graph Pad Prism 8.0 and 9.0 software package.

Results

Effects of STAT3 mutations on Y705 phosphorylation

To dissect the effects of LOF and GOF mutations in the DBD and SH2D of STAT3 on its functions, we first examined STAT3$^{-/-}$ MEF cells expressing either WT or mutant STAT3 to examine the impact of each mutation on cytokine-stimulated phosphorylation of STAT3 at Y705. In the absence of IL6 stimulation, basal levels of pY-STAT3 were higher in cells transfected with each of the 4 STAT3 GOF mutants compared with WT STAT3 transfected cells (Figure 1B and supplemental Figure 2). Levels of pY-STAT3 in IL6/soluble IL6 receptor (sIL6R)-stimulated cells bearing LOF DBD mutations, R382W, F384S, H437P, R423Q, and V463del, and the GOF DBD mutant, Q344H, were similar to those in cells transfected with WT STAT3 (Figure 1B-C). Except for N647D, the levels of pY-STAT3 in IL6/sIL6R-stimulated cells transfected with LOF SH2 mutations, S636Y, S668Y, T622I, Y657S, and V637M, were significantly reduced compared with cells transfected with WT STAT3. Notably, levels of pY-STAT3 in stimulated cells transfected with GOF SH2 mutants, Y640F, K658Y, and D661Y, were similar to those in stimulated cells transfected with WT STAT3 (Figure 1B-C). Levels of pY-STAT3 in STAT3$^{-/-}$ MEF cells coexpressing v-Src and WT or mutant STAT3 constructs corresponded to levels observed in each of their counterparts stimulated with IL6/sIL6R (supplemental Figure 3), indicating that mutation-induced alterations in pY-STAT3 levels were not limited to IL6/sIL6R-mediated STAT3 phosphorylation.

Effects of STAT3 mutations on STAT3 binding to pY-peptide ligand

Next, we asked whether LOF mutations affected STAT3 phosphorylation at pY705 downstream of IL6/sIL6R or v-Src by altering the ability of STAT3 to bind to phosphorylated sites on cognate receptors. We performed a pull-down assay on lysates of STAT3$^{-/-}$ MEF cells transfected with WT or mutant STAT3 constructs using neutravidin beads coated with either phosphorylated or unphosphorylated EGFR Y1068 biotinylated peptides.[22] Immunoblot analysis of the resulting eluates

showed that STAT3 proteins containing either GOF or LOF mutations within the DBD, Q344H, R382W, F384S, R423Q, H437P, and V463del, bound to immobilized pY1068 peptide to a similar extent as WT STAT3 (Figure 2A). However, nearly all the STAT3 proteins with mutations within the SH2D, including GOF mutations, Y640F and K658Y, and LOF mutations, T622I, S636Y, V637M, N647D, and Y657S, showed less binding to the pY1068 peptide compared with WT STAT3 (Figure 2A). These data suggest that reduced phosphorylation at Y705 of STAT3 proteins containing mutations within their SH2D is because of their decreased binding to pY-recruitment sites within activated signaling complexes. To confirm these findings and to more precisely quantify pY-peptide binding, we generated purified recombinant monomeric WT and mutant core STAT3 protein (residues 127-722) in bacteria (supplemental Figure 4) and assessed the binding of each protein to immobilized pY-peptide using SPR (Figure 2B and supplemental Figure 5A-B). Compared with WT STAT3 protein, STAT3 proteins containing either GOF or LOF mutations within the DBD, Q344H, R382W, F384S, R423Q, H437P, and V463del, showed modest reductions in binding to pY1068 peptide. In contrast, except for S668Y and N647D, the binding affinities of SH2D LOF mutants to pY-peptide were markedly decreased relative to WT (Figure 2B and supplemental Figure 5A-B). Similarly, the SH2D GOF mutants, such as the DBD LOF mutants, showed small reductions in binding affinities. Thus, diminished pY-peptide binding is a likely contributor to the reduced tyrosine phosphorylation of STAT3 proteins containing SH2D LOF mutations.

Effects of STAT3 mutations on cytokine-induced STAT3 homodimerization

Next, we developed a BRET-based assay to assess the effect of STAT3 mutations on cytokine-induced homodimerization.[25] For this assay, we generated WT and mutant STAT3 cDNA reporter constructs, NSF, and a negative control reporter construct, NLuc-WT STAT3 (NS), each of which contained nano-luciferase (NLuc), a highly stable and efficient luciferase enzyme,[26] at the N-terminus (Figure 3A). Except for the WT STAT3 negative control (NS), each of the reporter constructs contained an intramolecular FlAsH inserted immediately after residue 425 located within a loop in the DBD of STAT3. Based on the crystal structure of STAT3 homodimer bound to DNA, IL6/sIL6-induced homodimerization of the STAT3 WT NSF construct would be expected to juxtapose NLuc and FlAsH, resulting in a BRET signal (Figure 3B). We also generated 2 negative control NSF constructs that contained STAT3 mutations known to impair SH2-SH2 homodimerization: mutation R609K, which does not bind pY-peptide, and mutation Y705F, which eliminates canonical STAT3 Y705 phosphorylation.[5,27] When transfected into MEF cells, none of the NSF constructs, including the WT NSF construct, elicited a BRET signal in the absence of IL6/sIL6R (Figure 3C and supplemental Figure 6A). As expected, however, the WT NSF construct generated a readily detectable BRET signal in the presence of IL6/sIL6R, whereas the WT NS negative control reporter construct and the 2 NSF negative control mutation constructs, R609K and Y705, did not. STAT3 NSF constructs containing either DBD GOF or LOF mutations, Q344H, R382W, F384S, H437P, V463del, and R423Q, produced a BRET signal, indicating that their ability to form homodimers was similar to that of WT. In contrast, except
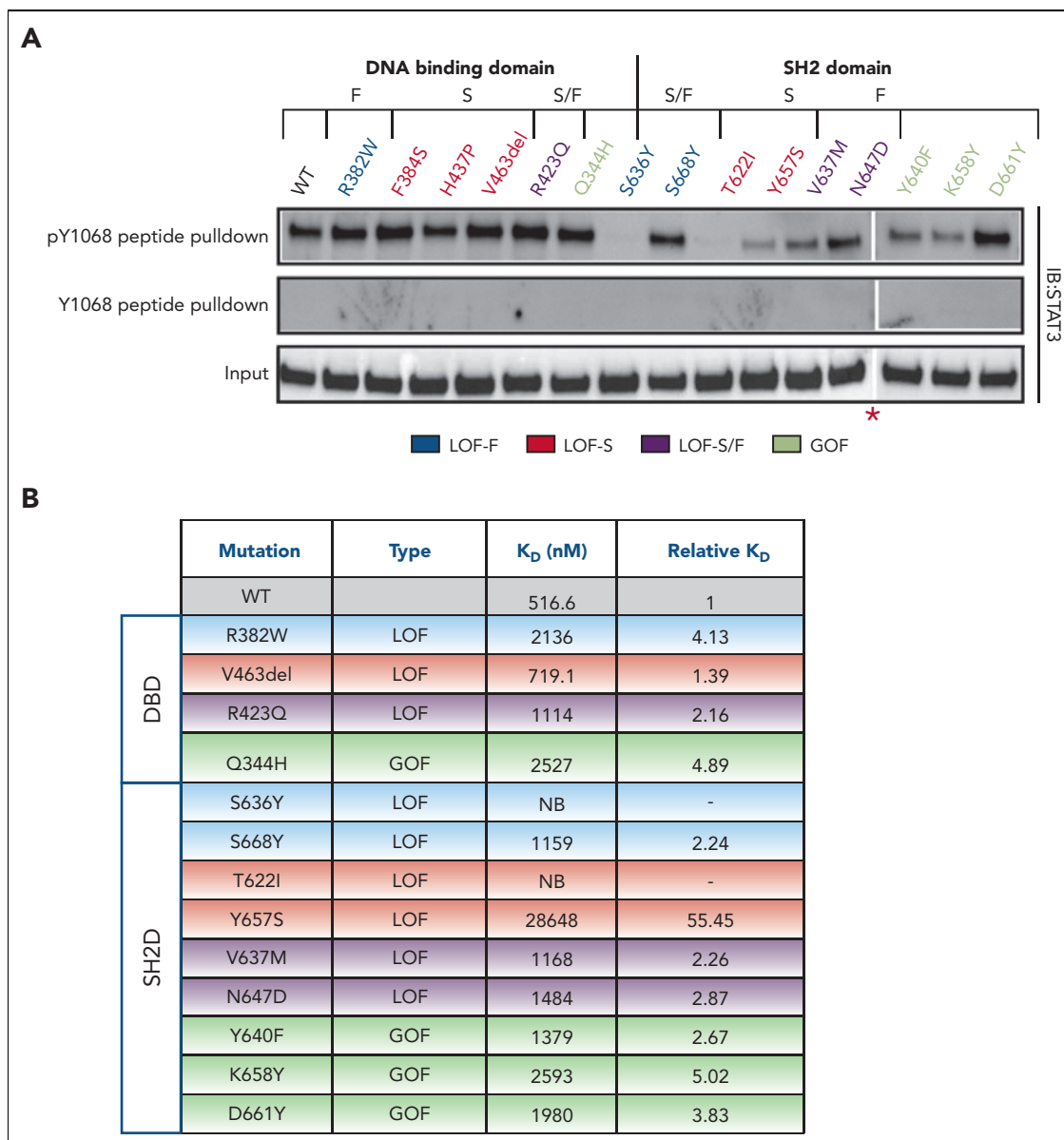
KASEMBELI et al

Figure 2. Effect of mutations on STAT3 binding to pY1068 dodecapeptide. (A) Biotinylated phosphorylated (p) Y1068 peptide or biotinylated nonphosphorylated Y1068 peptide (control) were immobilized onto streptavidin agarose beads and incubated with lysates of STAT3$^{-/-}$ MEF cells reconstituted with either WT or mutant STAT3 constructs. Bound proteins were separated by sodium dodecyl sulfate-polyacrylamide gel electrophoresis and immunoblotted with antibody against total STAT3. The red asterisk (*) indicates that the images are a composite of 2 separate blots imaged simultaneously with equal exposure. (B) SPR analysis of binding of WT and mutant core STAT3 (127-722) proteins to pY1068 peptide. K_D values were determined by fitting data to a 1-site equilibrium–binding model and the results shown are the mean of 3 experiments. Each K_D value was divided by the WT result of that experiment to determine the relative K_D value and the mean relative K_D of the 3 experiments shown; the dash (–) indicates the relative K_D could not be calculated. NB, no binding detected.

for N647D, STAT3 NSF constructs containing SH2D LOF mutations, S636Y, S668, T622I, Y657S, and V637M showed a significantly reduced BRET signal in the presence of IL6/sIL6R compared with WT STAT3. These data indicate that acquisition of a LOF mutation in the SH2D not only resulted in a reduced ability of STAT3 to be recruited to activated receptor complexes, but LOF mutant acquisition also resulted in a reduced ability to form homodimers. Intriguingly, although STAT3 SH2D GOF mutants formed homodimers, they showed a ~50% reduction in this ability compared with WT STAT3 (Figure 3C and supplemental Figure 6A).

To exclude the possibility that the increased BRET signal observed in the presence of IL6/sIL6R resulted from intramolecular rather than intermolecular interactions, we cotransfected cells with the WT STAT3 NSF construct and increasing amounts of the untagged WT STAT3 construct. We reasoned that if the increase in BRET signal generated by the NSF construct in response to IL6/sIL6R is owing to homodimer-induced intermolecular energy transfer, then an increase in untagged STAT3 should lead to a dose-dependent reduction in the BRET signal, which is what we observed (supplemental Figure 6B-D).
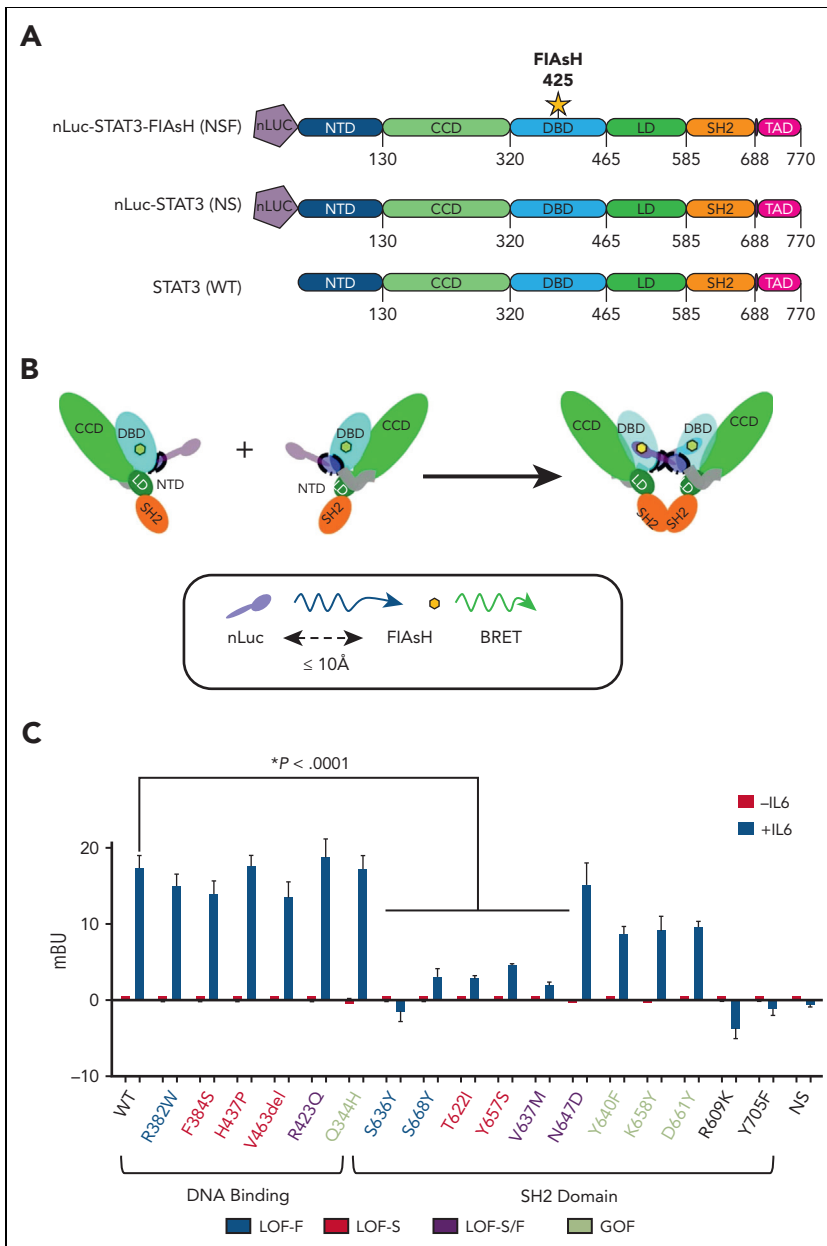
Figure 3. Effect of mutations on STAT3 homodimerization assessed using BRET reporter constructs. (A) STAT3 WT and mutant BRET constructs were generated that contained (NLuc inserted at the N-terminus of STAT3 and a FlAsH motif inserted within a flexible loop in the DBD immediately after residue 425 (NSF). A control STAT3 WT construct (NS) was generated that contained the NLuc but lacked the FlAsH motif. (B) A schematic of the mechanism for an increased BRET signal following STAT3 Y705 phosphorylation and homodimerization of an NSF construct is shown. (C) MEF$^{-/-}$ cells transiently transfected with the indicated NSF construct or control WT construct (NS) were incubated without or with IL6/sIL6R and used to measure intracellular mBU in real time. The mean ± SEM of 4 assays is shown (*$P < .0001$; Student t test). mBU, milli-BRET units.

Effects of STAT3 mutations on cytokine-induced nuclear localization of STAT3

To evaluate the effects of STAT3 LOF and GOF mutations in the DBD and SH2D on STAT3 nuclear translocation, we determined % NF in STAT3$^{-/-}$ MEF cells transfected with WT or mutant Ac-GFP1-STAT3 constructs and incubated without or with IL6/sIL6R, as described.[28] The %NF in IL6/sIL6R-stimulated cells expressing the STAT3 GOF mutation, Q344H, or each of the DBD LOF mutations, R382W, F384S, H437P, V463del, and R423W, were indistinguishable from cells expressing WT STAT3 (Figure 4A-B), as was the %NF in IL6/sIL6R-stimulated cells expressing each of the STAT3 SH2D GOF. However, except for N647D, the %NF in IL6/sIL6R-stimulated cells expressing each of the SH2D LOF mutants, T622I, S636Y, V637M, Y657S, and S668Y, was reduced by 40% or more compared with WT STAT3 (Figure 4B). Thus, nuclear translocation correlated well with levels of STAT3 Y705 phosphorylation and homodimerization.

Effects of STAT3 mutations on STAT3 binding to DNA

To evaluate the effects of STAT3 mutations on STAT3 binding to DNA, we expressed and purified phosphorylated STAT3 (127-722) homodimer proteins from bacteria transformed with either WT or mutant core STAT3 constructs. The dimeric state of each protein was verified by gel chromatography, native PAGE, and crosslinking experiments (supplemental Figure 4A-D) before measuring DNA-binding affinity using an SPR assay.[29] Each homodimer containing a LOF mutation, regardless of its location within either the DBD or SH2D, showed reduced affinity for duplex DNA compared with WT (Figure 5A-B and supplemental Figure 7). Notably, the DBD LOF mutants, R382W and V463del, and the SH2 LOF mutant, Y657S, showed a complete loss of DNA-binding activity. In contrast, the SH2D GOF mutants, Y640F, K658Y, and D661Y, showed an increase in the DNA-binding affinity
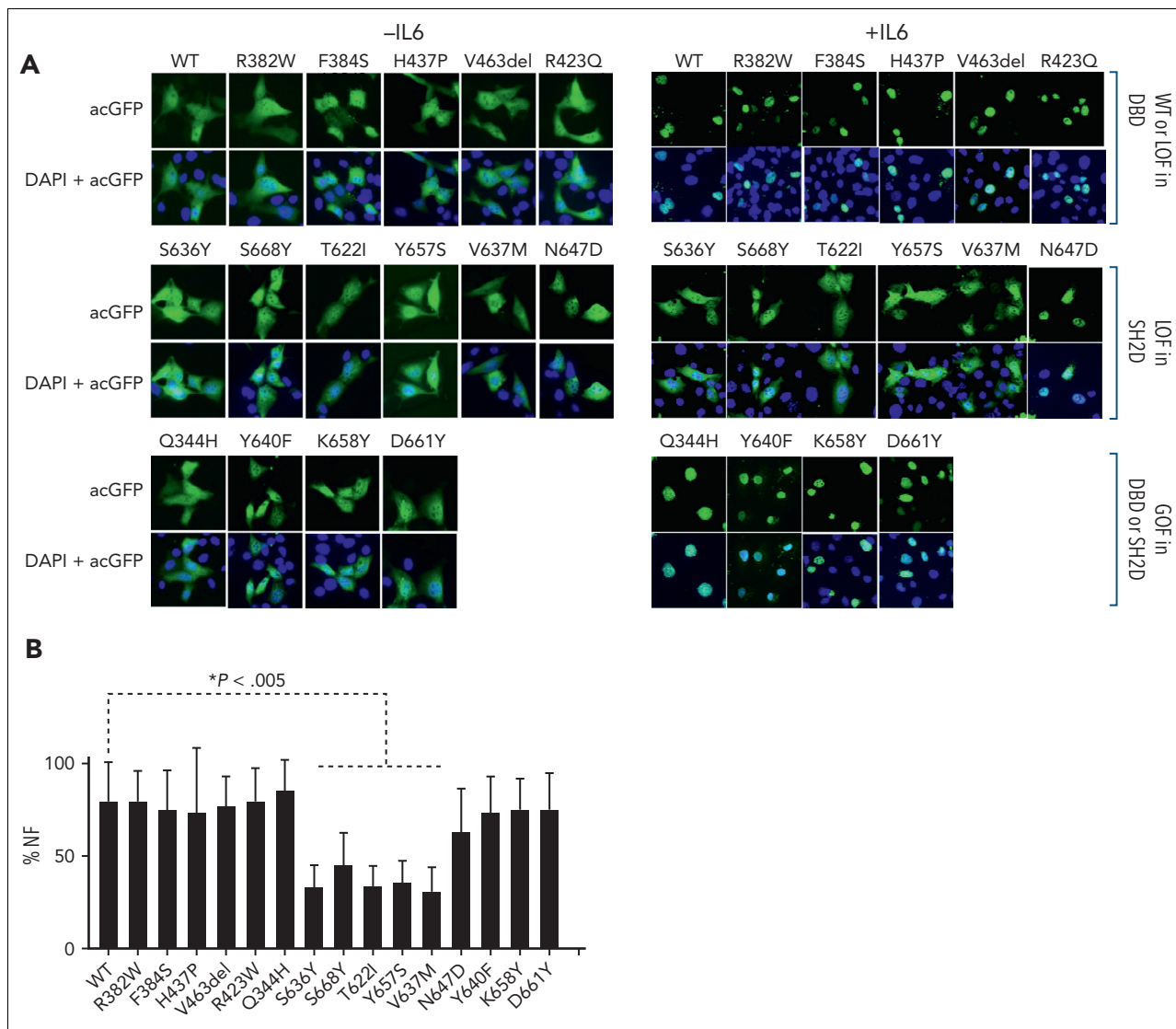
Figure 4. Effect of mutations on cytokine-induced nuclear localization of STAT3. (A) STAT3$^{-/-}$ MEF cells were transiently transfected with Ac-GFP1–tagged WT or mutant STAT3 expression constructs and incubated without (left panels) or with (right panels) IL6/sIL6R. Cells were fixed, stained with DAPI, and examined by fluorescence microscopy; representative fields are shown. (B) The % FN in cells was calculated for 30 to 40 cells incubated with IL6/sIL6R and the mean ± SEM of 3 assays is shown (*P < .005; Student *t* test).

compared with the WT homodimer (Figure 5A-B and supplemental Figure 7).

Next, we examined lysates of STAT3$^{-/-}$ MEF cells expressing full-length STAT3 WT and mutant constructs for DNA-binding activity following IL6/IL6R stimulation using an ELISA-based DNA-binding assay (Figure 5C). Similar to the SPR results, each of the LOF mutants, irrespective of their location within the DBD or SH2D, showed reduced binding to DNA than WT STAT3, whereas the SH2D GOF mutants, Y640F, K658Y, and D661Y, showed markedly increased DNA binding than WT STAT3.

Effects of STAT3 mutations on the conformational stability of STAT3 monomers and homodimers

Although a protein's specific functions are determined by its 3D structure, the strength and duration of its functions are determined, at least in part, by its conformational stability. Our previous results suggested that some LOF mutations reduce the conformational stability of STAT3.[13] To determine directly if mutations in STAT3 affected protein stability, we determined the thermal unfolding of WT and mutant STAT3 proteins using differential scanning fluorometry.[17] The peak of the first derivative of the fluorescent signal vs temperature (dF/dT) represents the melting temperature (T_m) of the protein. A shift in the T_m of a mutant protein compared with WT protein indicates that the mutant protein is either less stable (left shift) or more stable (right shift) than WT protein. Examination of monomeric STAT3 WT and DBD LOF mutant proteins showed a small decrease in T_m for mutants R382W and V463del but not mutant R423Q, compared with WT ($\Delta T_m = -0.3$ to $-2°C$) indicating decreased conformational stability of 2 of 3 of the DBD LOF STAT3 mutant monomer proteins (Figure 6A-D and supplemental Figure 8). In contrast, except for Y640F and N647D, STAT3 SH2D mutant monomers showed a greater decrease in the T_m than WT
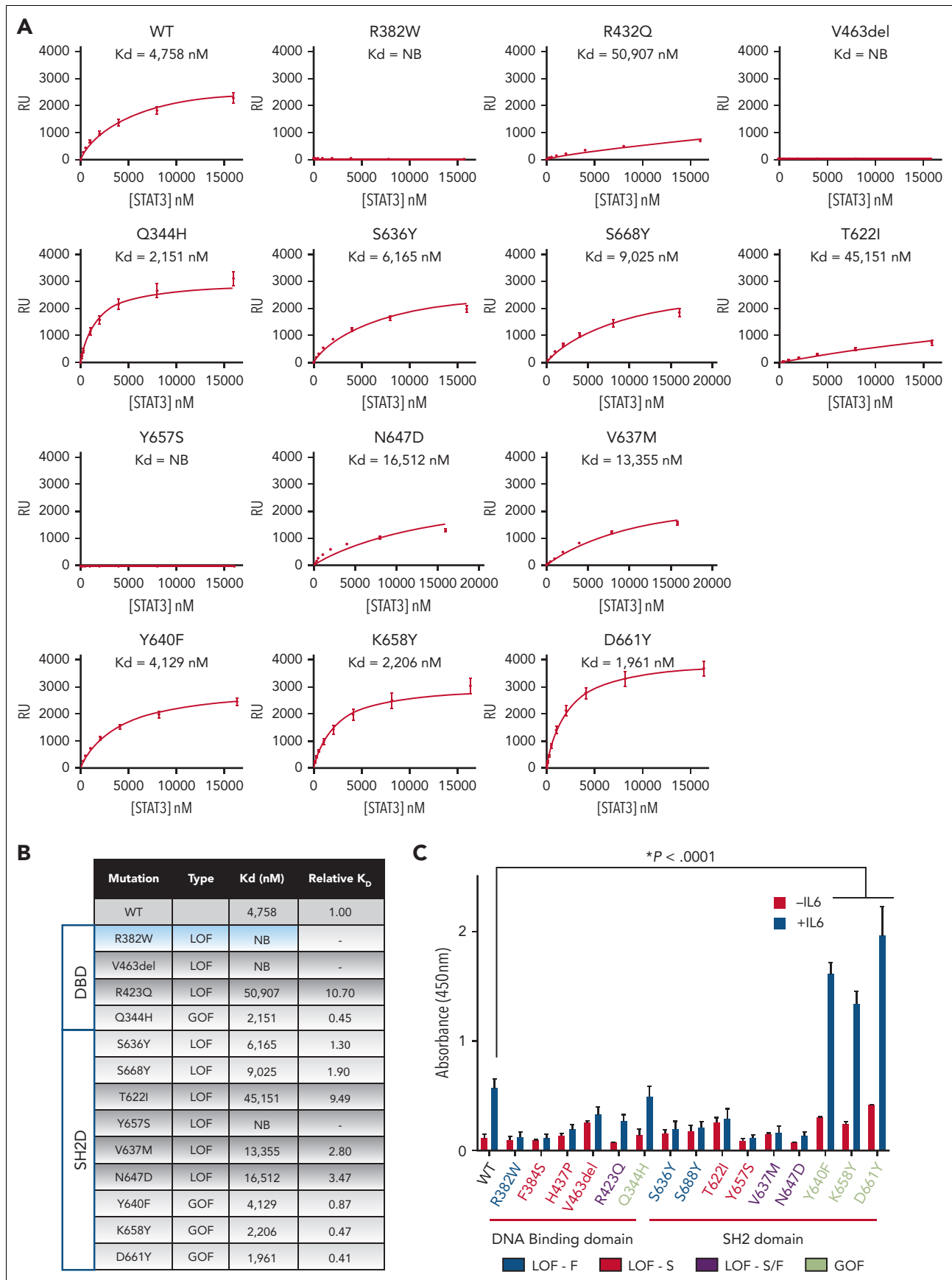
Figure 5. Effect of mutations on STAT3 homodimer binding to DNA. (A) WT or mutant pY-STAT3 homodimers that were expressed and purified from bacteria were analyzed for binding to immobilized duplex hSIE DNA by SPR. Equilibrium RU values shown were calculated from sensograms shown in supplemental Figure 7 and plotted

monomer (ΔT_m = −2 to −8°C), regardless of whether they were GOF or LOF mutants (Figure 6A-D).

We next assessed the effect of homodimerization on the thermal unfolding of WT and mutant STAT3 proteins. The T_m of WT STAT3 homodimers (66°C) was 11°C higher than that of WT STAT3 monomers (55°C), indicating that homodimerization substantially increases the conformational stability of STAT3 (Figure 6A-D and supplemental Figure 8). Similarly, the T_m of each homodimer of mutant STAT3 protein was higher than its monomer counterpart by +2 to +11°C. However, homodimers of SH2D LOF mutants showed a smaller increase in T_m than WT, indicating less improvement in their conformational stability with homodimerization compared with WT STAT3.

Importantly, instead of showing a single transition melting point as seen with WT and protein homodimers, the unfolding curves of the SH2D GOF mutant homodimers were biphasic with 2 transition melting points designated T_m1 and T_m2 (Figure 6A-D and supplemental Figure 8) ranging from 55.3 to 59.0°C and 76 to 78°C, respectively. In addition, although the ΔT_m1 for GOF SH2D mutant proteins ranged from −6.3 to −10.7°C, the ΔT_m2 for these mutants ranged from +10 to +12°C. These findings strongly suggest that the predominant effect of SH2D GOF mutations contributing to their enhanced DNA binding is the increased conformational stability of their homodimers, but not their monomers. In addition, it appears likely that homodimers of SH2D GOF mutant STAT3 proteins unfold via a dimeric intermediate.

A STAT3 inhibitor, TTI-101, blocks protein binding to pY-peptide and cell growth driven by STAT3 GOF mutants

We previously identified TTI-101, a small-molecule STAT3 inhibitor that targets the pY-peptide–binding pocket within the STAT3 SH2D[23,24]; TTI-101 is currently undergoing phase II testing in patients with cancer.[30,31] To determine whether STAT3 SH2D GOF mutants identified in patients with lymphoma are sensitive to the inhibitory effects of TTI-101 or if they have acquired resistance to TTI-101 as a result of having a mutation within the same domain targeted by TTI-101, we first performed SPR assays. TTI-101 reduced the binding to pY1068 dodecapeptide of 3 of the most common STAT3 SH2D GOF mutant proteins, Y640F, K658Y, and D661Y, with IC_{50} values of 1.78, 0.82, and 3.13 μM, respectively, which were within 1.2- to 4.7-fold of the IC_{50} for TTI-101's inhibition of binding by WT STAT3 protein (0.66 μM; Figure 7A).

To determine if TTI-101 also inhibits cell growth driven by STAT3 SH2D GOF mutants, STAT3$^{-/-}$ MEF cells were stably transfected with empty pAcGFP1-C1 vector, or with pAcGFP1-C1 vector encoding WT STAT3 or the D661Y GOF mutant (supplemental Figure 9A). Under low-serum conditions (0.5% FBS; supplemental Figure 9B) and no-serum conditions (data not shown), the number of vector control cells did not increase, whereas the number of cells stably expressing either WT STAT3 or STAT3 GOF mutant D661Y did increase. TTI-101 inhibited

cell growth driven by the D661Y mutant (IC_{50} = 0.9 ± 0 μM) to the same extent as it inhibited growth driven by WT STAT3 (IC_{50} = 1.9 ± 0.6 μM) in 0.5% FBS (Figure 7B), as well as in 0% FBS (WT STAT3 IC_{50} = 1.0 ± 0.8 μM; D661Y IC_{50} = 0.7 ± 0.1 μM, Figure 7C). These findings support the possibility of using TTI-101 in the treatment of patients with cancers caused by STAT3 SH2D GOF mutations.

Discussion

Our detailed biophysical, biochemical, and cellular analyses of STAT3 mutants causing AD-HIES and cancer showed distinct repertoires of alterations in critical STAT3 activation steps and functions based on the domain location and classification of the mutations as LOF or GOF (Table 1). Compared with WT STAT3, DBD LOF mutants had impaired DNA binding and a minor defect in pY-peptide binding that was uncovered in SPR assays performed on the core STAT3 protein (127-688). The DBD GOF mutant, Q344H, demonstrated increased DNA-binding affinity in SPR assays, higher levels of constitutive tyrosine phosphorylation, but slightly reduced pY-peptide binding in SPR assays, similar to DBD LOF mutants. Compared with WT STAT3, SH2D LOF mutants showed reduction in the following: (1) pY-STAT3 levels induced by IL6/sIL6R or v-SRC, (2) pY-peptide binding in both pull-down and SPR assays, (3) homodimerization, (4) nuclear accumulation, and (5) DNA binding in both SPR assays and ELISAs. Compared with WT STAT3, SH2D GOF mutants showed increased DNA binding by SPR (2/3 mutants) and by ELISA (3/3 mutants). Importantly, mutation-induced changes in conformational stability of mutant protein monomers, homodimers, or both can explain the alterations in STAT3 activation steps and/or functions observed in STAT3 SH2D mutants causing AD-HIES or cancer. The reduced pY-peptide binding, phosphorylation, homodimerization, nuclear localization, and DNA binding observed in STAT3 SH2D LOF mutants that cause AD-HIES are linked to the reduced global conformational stability of both their monomers and homodimers. In contrast, the increased global conformational stability of their homodimers explains enhanced DNA binding by STAT3 SH2D GOF mutants.

The reduced DNA binding observed in DBD LOF mutants does not appear to be because of reduced global conformational stability of their monomers and/or homodimers, rather, to domain-limited structural alterations that reduce DBD-specific functions. Reduced DNA binding of these mutants also was dominant-negative, as DNA binding in cells that coexpressed a STAT3 DBD LOF mutant protein and STAT3 WT protein was decreased below the level expected from a dose-effect reduction in fully functional STAT3 (supplemental Figure 10). These results confirm a recent report[32] that many, if not all, AD-HIES mutations function as dominant negatives. The increased DNA binding observed in the DBD GOF mutation, Q344H, is not explained by improved stability of either its monomer and/or homodimer but by enhancement of the electrostatic interactions of mutant STAT3 homodimers with the DNA duplex caused by substitution of the polar, but uncharged, Q with the positively charged H (supplemental Figure 11).

Figure 5 (continued) against STAT3 protein concentration. (B) K_D values were determined by fitting the data to a 1-site equilibrium–binding model. The results shown are the mean of 6 experiments. Each K_D value was divided by the WT result for that experiment to determine the relative K_D value and the mean relative K_D of the 6 experiments shown; the dash (–) indicates the relative K_D could not be calculated. (C) Protein lysates of STAT3$^{-/-}$ MEF cells that expressed Ac-GFP1–tagged WT or mutant STAT3α and incubated without or with IL6/sIL6R were examined using the TransAM STAT3 DNA-binding assays. The mean ± SEM of 3 assays is shown (*P < .0001; Student t test).
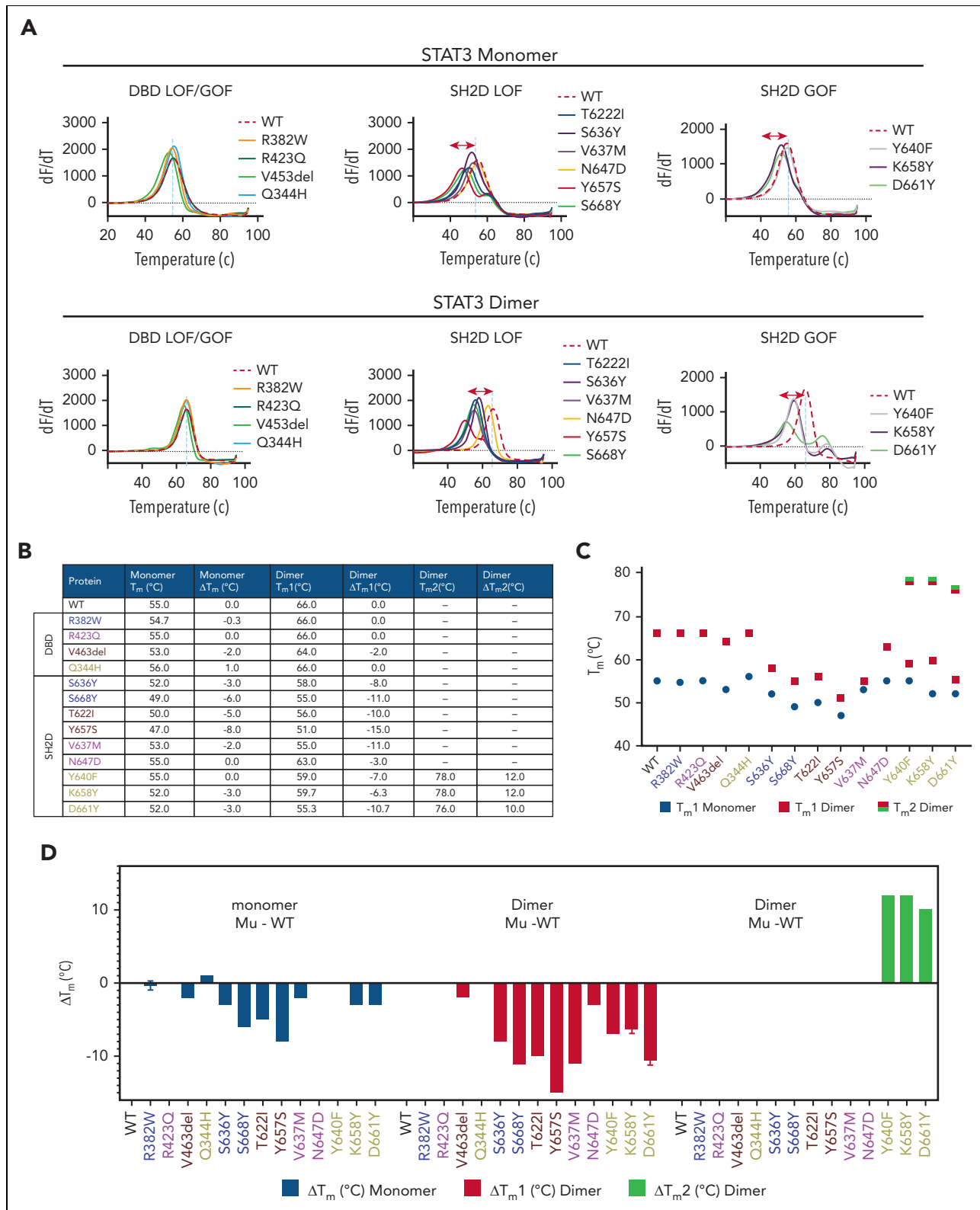
Figure 6. Effect of mutations on thermal stability of STAT3 protein monomers and homodimers. (A) Bacterially expressed and purified WT and mutant STAT3 proteins were examined for thermal stability using the differential scanning fluorimetry assay; change in fluorescence (dF) is recorded with increasing temperature (dT). The first derivative of each melting curve (dF/dT) is shown for WT and mutants organized into mutant categories and examined as monomers (right panels) or as homodimers (left panels). The inflection point or T_m for WT STAT3 monomers and homodimers is indicated by the vertical dashed line in each panel. (B-D) The calculated T_m of each mutant monomer, the primary T_m (T_m1) and secondary T_m (T_m2) of each GOF SH2D mutant homodimer, and the differences between the T_m, T_m1, or T_m2 of each mutant and the corresponding T_m of WT STAT3 (ΔT_m) are shown in tabular form (B) and graphically (C-D).
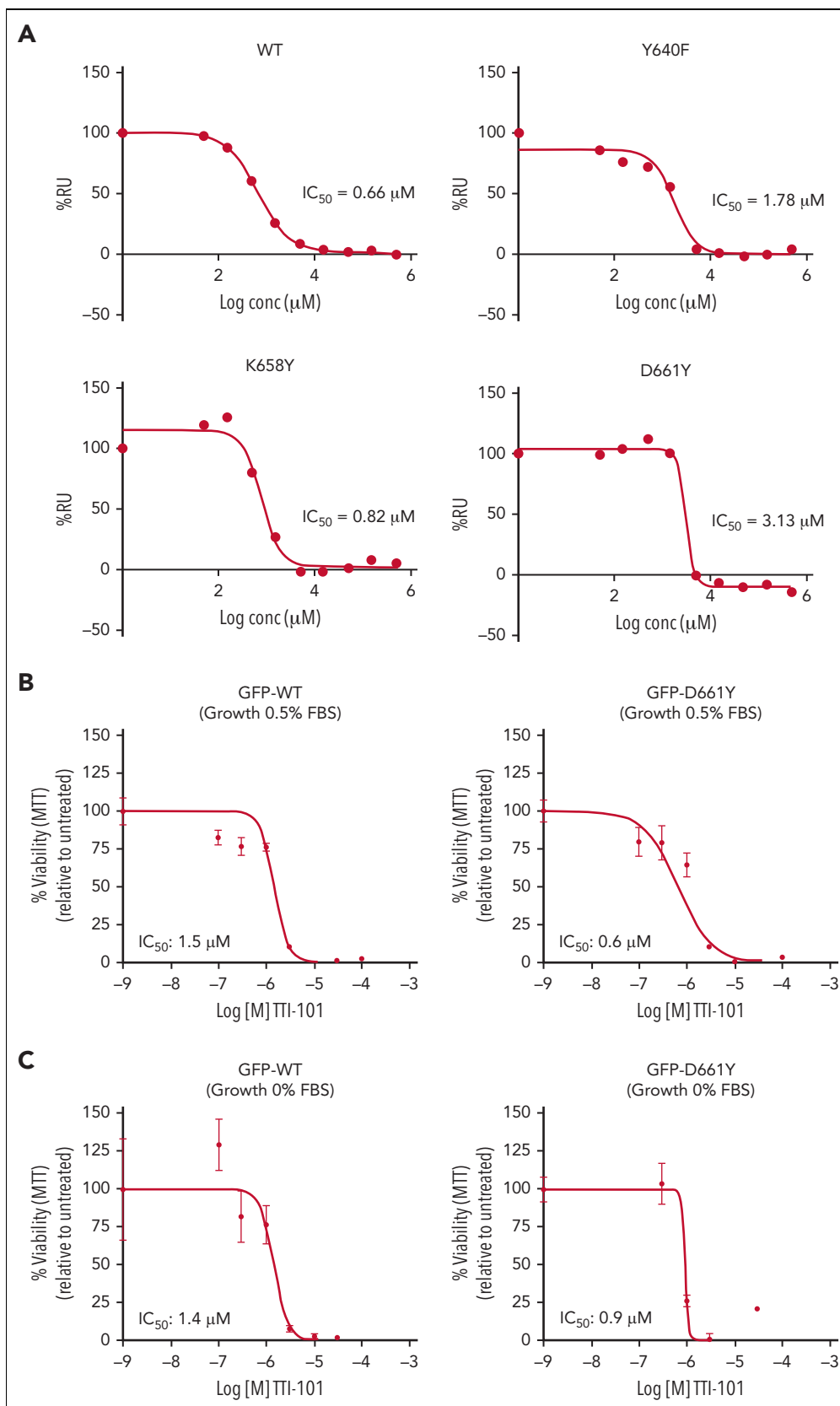
Figure 7. Effect of TTI-101 on pY-peptide binding in vitro and on STAT3-dependent growth in vivo of WT or STAT3 SH2D GOF mutants. (A) IC_{50} of TTI-101 inhibition of binding of STAT3 WT or GOF mutant protein to pY1086-peptide measured by SPR. (B-C) Representative IC_{50} curves of 2 experiments each showing TTI-101 inhibition of growth of STAT3$^{-/-}$ MEF cells stably transfected with WT (left) or the STAT SH2D GOF mutant, D661Y (right) and grown in medium with 0.5% FBS (B) or in media with 0% serum (C).

Table 1. Summary of results with WT and mutant STAT3 proteins

STAT3 protein	WT	R382W	F384S	H437P	V463del	R423Q	Q344H	S636Y	S668Y	T6221	Y657S	V637M	N647D	Y640F	K658Y	D661Y
Domain	NA	DBD						SH2D								
Classification—LOF vs GOF	NA	LOF					GOF	LOF						GOF		
Classification—F, S, or S/F	NA	F	S	S	S	S/F	NA	F	F	S	S	S/F	S/F	NA	NA	NA
pY-STAT3—w/o IL6/sIL6R	-	-	-	-	-	-	+	-	-	-	-	-	-	+	+	+
pY-STAT3—with IL6/sIL6R	+++	+++	+++	+++	+++	+++	+++	+	++	++	++	++	+++	+++	+++	+++
pY-STAT3—with v-Src	+++	+++	+++	+++	+++	+++	+++	+	+	+	+	+	+	+++	+++	+++
pY1068—pull-down	+++	+++	+++	+++	+++	+++	+++	-	++	-	+	+	++	+	+	+++
pY1068—SPR	+++	+	ND	ND	++	++	+	-	++	-	-	+	+	+	+	+
Homodimerization	+++	+++	+++	+++	+++	+++	+++	-	+	+	+	+	+++	++	++	++
Nuclear accumulation	++	++	++	++	++	++	++	+	+	+	+	+	++	++	++	++
DNA binding—SPR	+++	-	ND	ND	-	-	++++	++	++	+	-	++	++	+++	++++	++++
DNA binding—ELISA	++	-	-	-	-	+	++	-	-	-	-	-	-	++++	++++	++++

F, functional; NA, not applicable; ND, not done; S, structural; S/F, structural-functional.[22]

Our studies showed a small but consistent finding of reduced pY-peptide binding in SPR assays of both the DBD LOF and GOF mutants, suggesting that mutations in the DBD may have a deleterious allosteric effect on this SH2D function, which has been demonstrated for mutations that occur in other domains of STAT3, notably the coil-coiled domain and linker domain.[33,34] Defects in STAT3 functions downstream of pY-peptide binding, such as STAT3 Y705 phosphorylation, homodimerization, and nuclear accumulation, however, were not observed in DBD LOF mutants. As for DBD GOF mutants, the reduced recruitment to pY-peptide would be expected to be more than compensated for by the enhanced ability of these mutants to bind DNA.

SH2D LOF mutation N647D demonstrated the fewest defects among the SH2D LOF mutants, exhibiting only reduced pY-peptide binding by pull-down and SPR and reduced DNA binding by SPR and ELISA. Based on our previous in silico analyses (supplemental Figure 11), mutations at residue N647 were designated as structural-functional. However, data generated here suggest that N647 plays a purely functional role in dimer formation and has minimal contribution to the thermodynamic stability of STAT3.

Thermal stability curves indicated that, except for SH2D GOF mutant proteins, each STAT3 monomer and homodimer protein examined in this study unfolded in a single step with no intermediates, which suggests their unfolding is cooperative. Although the unfolding of monomers of the 3 SH2D GOF mutant proteins also was monophasic, the unfolding curve of each of their homodimers was biphasic, which suggests that their homodimer unfolding is not cooperative and that it proceeds through an intermediate that likely is a dimer that has increased stability. Increased stability of SH2D GOF STAT3 mutant proteins is associated with improved DNA-binding activity (Figure 5), as well as higher levels of constitutive pY-STAT3 (supplemental Figure 2) owing to the reduced rates of dephosphorylation.[35]

A unique aspect of STAT protein signaling is that its recruitment to activated receptor complexes and its dimerization share the same mechanism, that is, binding of the STAT SH2 domain to a pY-peptide ligand. For the process of STAT signaling to proceed, homodimerization would be expected to be favored energetically over receptor binding. Here, we show that the STAT3 homodimer structure is more stable energetically than the STAT3 monomer structure. The greater stability of STAT3 homodimer than monomer may drive the transition from STAT3 monomers to homodimers and, thus, be a major determinant of STAT3 signal transduction. Greater stability of homodimers than monomer would be expected to drive the signal transduction pathways of other members of the STAT protein family.

We previously showed that small-molecule modulators of proteostasis, including one currently in clinical use, have the potential to restore STAT3 activity in cells containing STAT3 LOF mutants that cause AD-HIES.[13] Here, we show that TTI-101, a small-molecule STAT3 inhibitor[24,36,37] that targets the SH2D of STAT3 and has entered phase II studies in patients with cancer, blocked binding of cancer-causing STAT3 SH2D GOF mutant proteins to pY-peptide, as well as reduced STAT3-dependent cell growth of STAT3$^{-/-}$ MEF cells reconstituted with STAT3 GOF mutant, D661Y. TTI-101's inhibition of cell growth driven by this mutant likely results, in part, from its ability to destabilize D661Y homodimers, leading to reduced DNA binding. Thus, one of the principal implications of our study is that STAT3 protein stability is a major determinant of the pathogenesis of diseases caused by STAT3 SH2D LOF and GOF mutations. Furthermore, agents that increase or decrease STAT3 protein stability may be useful in the treatment of diseases caused by STAT3 LOF or GOF mutations, respectively.

Authorship

Contribution: M.M.K. proposed the hypotheses, designed the study, either performed or oversaw the performance of the experiments, analyzed study data, and wrote the manuscript; U.B. designed the study, performed the experiments, analyzed data, and wrote the manuscript; E.K., A.A., A.K., and B.A. performed experiments and analyzed data; and D.J.T. proposed the hypotheses, designed the study, interpreted data, and wrote the manuscript.

Conflict-of-interest disclosure: Baylor College of Medicine, with D.J.T. as inventor, filed patents covering the use of TTI-101, a small-molecule inhibitor of STAT3 used in this study. These patents are exclusively licensed to Tvardi Therapeutics, Inc. D.J.T. receives compensation as a member of Tvardi Therapeutics' scientific advisory board and holds equity in the company. The University of Texas MD Anderson Cancer Center has an institutional financial conflict of interest with Tvardi Therapeutics, Inc related to the research being reported in this manuscript. D.J.T., Division Head of Internal Medicine, also has a financial interest with Tvardi Therapeutics. Because MD Anderson is committed to the protection of human subjects and the effective management of its financial conflicts of interest in relation to its research activities, MD Anderson has implemented an Institutional Conflict of Interest Management and Monitoring Plan (Plan) to manage and monitor the conflict of interest with respect to MD Anderson's conduct of this research. The remaining authors declare no competing financial interests.

ORCID profiles: E.K., 0000-0003-2611-7648; U.B., 0000-0002-8676-7258; D.J.T., 0000-0001-8492-8460.

Correspondence: David J. Tweardy, Division of Internal Medicine, The Department of Infectious Diseases, Infection Control & Employee Health, University of Texas MD Anderson Cancer Center, 1515 Holcombe Blvd, Houston, TX 77030-4009; email: djtweardy@mdanderson.org.

Footnotes

REFERENCES

1. Bharadwaj U, Kasembeli MM, Robinson P, Tweardy DJ. Targeting Janus kinases and signal transducer and activator of transcription 3 to treat inflammation, fibrosis, and cancer: rationale, progress, and caution. *Pharmacol Rev.* 2020;72(2):486-526.

2. Jin W. Role of JAK/STAT3 signaling in the regulation of metastasis, the transition of cancer stem cells, and chemoresistance of cancer by epithelial-mesenchymal transition. *Cells.* 2020;9(1):217.

3. Yu H, Lee H, Herrmann A, Buettner R, Jove R. Revisiting STAT3 signalling in cancer: new and unexpected biological functions. *Nat Rev Cancer.* 2014;14(11):736-746.

4. Darnell JE Jr, Kerr IM, Stark GR. Jak-STAT pathways and transcriptional activation in response to IFNs and other extracellular signaling proteins. *Science.* 1994;264(5164): 1415-1421.

5. Becker S, Groner B, Muller CW. Three-dimensional structure of the Stat3beta homodimer bound to DNA. *Nature.* 1998; 394(6689):145-151.

6. Minegishi Y, Saito M, Tsuchiya S, et al. Dominant-negative mutations in the DNA-binding domain of STAT3 cause hyper-IgE syndrome. *Nature.* 2007;448(7157):1058-1062.

7. Ohgami RS, Ma L, Monabati A, Zehnder JL, Arber DA. STAT3 mutations are present in aggressive B-cell lymphomas including a subset of diffuse large B-cell lymphomas with CD30 expression. *Haematologica.* 2014; 99(7):e105-107.

8. Zhu F, Wang KB, Rui L. STAT3 activation and oncogenesis in lymphoma. *Cancers.* 2019;12(1): 19.

9. Jägle S, Heeg M, Grün S, et al. Distinct molecular response patterns of activating STAT3 mutations associate with penetrance of lymphoproliferation and autoimmunity. *Clin Immunol.* 2020;210:108316.

10. Milner JD, Vogel TP, Forbes L, et al. Early-onset lymphoproliferation and autoimmunity caused by germline STAT3 gain-of-function mutations. *Blood.* 2015;125(4):591-599.

11. Faletti L, Ehl S, Heeg M. Germline STAT3 gain-of-function mutations in primary immunodeficiency: impact on the cellular and clinical phenotype. *Biomed J.* 2021;44(4): 412-421.

12. Kasembeli M, Lau WC, Roh SH, et al. Modulation of STAT3 folding and function by TRiC/CCT chaperonin. *PLoS Biol.* 2014;12(4): e1001844.

13. Bocchini CE, Nahmod K, Katsonis P, et al. Protein stabilization improves STAT3 function in autosomal dominant hyper-IgE syndrome. *Blood.* 2016;128(26):3061-3072.

14. Greeley N. *Mutations in STAT3 associated with human hyper IgE syndrome enhance NFκB and MAPK-mediated gene expression.* Thesis. The University of Texas Graduate School of Biomedical Sciences at Houston; 2012.

15. Mohr A, Fahrenkamp D, Rinis N, Müller-Newen G. Dominant-negative activity of the STAT3-Y705F mutant depends on the N-terminal domain. *Cell Commun Signal.* 2013;11:83.

16. Domoszlai T, Martincuks A, Fahrenkamp D, Schmitz-Van de Leur H, Küster A, Müller-Newen G. Consequences of the disease-related L78R mutation for dimerization and activity of STAT3. *J Cell Sci.* 2014;127(Pt 9): 1899-1910.

17. Niesen FH, Berglund H, Vedadi M. The use of differential scanning fluorimetry to detect ligand interactions that promote protein stability. *Nat Protoc.* 2007;2(9): 2212-2221.

18. Todaro F, Tamassia N, Pinelli M, et al. Multisystem autoimmune disease caused by increased STAT3 phosphorylation and dysregulated gene expression. *Haematologica.* 2019;104(7):e322-e325.

19. Kim D, Park G, Huuhtanen J, et al. STAT3 activation in large granular lymphocyte leukemia is associated with cytokine signaling and DNA hypermethylation. *Leukemia.* 2021; 35:3430-3443.

20. Becker S, Corthals GL, Aebersold R, Groner B, Muller CW. Expression of a tyrosine phosphorylated, DNA binding Stat3beta dimer in bacteria. *FEBS Lett.* 1998;441(1): 141-147.

21. Costa-Pereira AP, Tininini S, Strobl B, et al. Mutational switch of an IL-6 response to an interferon-gamma-like response. *Proc Natl Acad Sci U S A.* 2002;99(12):8043-8047.

22. Shao H, Xu X, Mastrangelo M-AA, et al. Structural requirements for signal transducer and activator of transcription 3 binding to phosphotyrosine ligands containing the YXXQ motif. *J Biol Chem.* 2004;279(18): 18967-18973.

23. Xu X, Kasembeli MM, Jiang X, Tweardy BJ, Tweardy DJ. Chemical probes that competitively and selectively inhibit Stat3 activation. *PLoS One.* 2009;4(3):e4783.

24. Bharadwaj U, Eckols TK, Xu X, et al. Small-molecule inhibition of STAT3 in radioresistant head and neck squamous cell carcinoma. *Oncotarget.* 2016;7(18):26307-26330.

25. Borroto-Escuela DO, Flajolet M, Agnati LF, Greengard P, Fuxe K. Bioluminescence resonance energy transfer methods to study G protein-coupled receptor-receptor tyrosine kinase heteroreceptor complexes. *Methods Cell Biol.* 2013;117:141-164.

26. England CG, Ehlerding EB, Cai W. NanoLuc: a small luciferase is brightening up the field of bioluminescence. *Bioconjugate Chem.* 2016; 27(5):1175-1187.

27. Mayer BJ, Jackson PK, Baltimore D. The noncatalytic src homology region 2 segment of abl tyrosine kinase binds to tyrosine-phosphorylated cellular proteins with high affinity. *Proc Natl Acad Sci U S A.* 1991;88(2): 627-631.

28. Kelley JB, Paschal BM. Fluorescence-based quantification of nucleocytoplasmic transport. *Methods.* 2019;157:106-114.

29. Minus MB, Liu W, Vohidov F, et al. Rhodium(II) proximity-labeling identifies a novel target site on STAT3 for inhibitors with potent anti-leukemia activity. *Angew Chem Int Ed Engl.* 2015;54(44):13085-13089.

30. Tsimberidou AM, de Achaval S, Alibhai I, Kaseb AO. First-in-man phase I clinical trial evaluating TTI-101, an orally bioavailable, small molecule inhibitor of STAT3, in patients with advanced solid tumors. *J Clin Oncol.* 2021;39(15_suppl):TPS3158-TPS3158.

31. Oral STAT3 inhibitor, TTI-101, in patients with advanced cancers. ClinicalTrials.gov identifier: NCT03195699. Updated 19 October 2022. Accessed 21 September 2022. https://clinicaltrials.gov/ct2/show/ NCT03195699

32. Asano T, Khourieh J, Zhang P, et al. Human STAT3 variants underlie autosomal dominant hyper-IgE syndrome by negative dominance. *J Exp Med.* 2021;218(8):e20202592.

33. Zhang T, Kee WH, Seow KT, Fung W, Cao X. The coiled-coil domain of Stat3 is essential for its SH2 domain-mediated receptor binding and subsequent activation induced by epidermal growth factor and interleukin-6. *Mol Cell Biol.* 2000;20(19):7132-7139.

34. Mertens C, Haripal B, Klinge S, Darnell JE. Mutations in the linker domain affect phospho-STAT3 function and suggest targets for interrupting STAT3 activity. *Proc Natl Acad Sci U S A.* 2015;112(48):14811-14816.

35. Yang J, Kunimoto H, Katayama B, et al. Phospho-Ser727 triggers a multistep inactivation of STAT3 by rapid dissociation of pY705-SH2 through C-terminal tail modulation. *Int Immunol.* 2020;32(2): 73-88.

36. Jung KH, Yoo W, Stevenson HL, et al. Multifunctional effects of a small-molecule STAT3 inhibitor on NASH and hepatocellular carcinoma in mice. *Clin Cancer Res.* 2017; 23(18):5537-5546.

37. Wei W, Tweardy DJ, Zhang M, et al. STAT3 signaling is activated preferentially in tumor-initiating cells in claudin-low models of human breast cancer. *Stem cells.* 2014; 32(10):2571-2582.